(2,4,6-Tris(trifluoromethyl)phenyl)palladium(II) Complexes

Camino Bartolomé, Pablo Espinet,*,† and Fernando Villafañe

Departamento de Química Inorgánica, Facultad de Ciencias, Universidad de Valladolid, 47005 Valladolid, Spain

Sabine Giesa, Antonio Martín, and A. Guy Orpen‡

School of Chemistry, University of Bristol, Bristol BS8 1TS, U.K.

Received October 27, 1995⊗

Complexes containing one or two Fmes ligands (Fmes = 2,4,6-tris(trifluoromethyl)phenyl = nonafluoromesityl) either *trans* or *cis* are obtained by treating palladium(II) chloro complexes with Li(Fmes): *trans*-$[PdCl_2L_2]$ (L = tetrahydrothiophene (tht), PPh_3) lead to *trans*-$[Pd(Fmes)ClL_2]$ (L = tht, PPh_3) or *trans*-$[Pd(Fmes)_2L_2]$ (L = tht); $[PdCl_2(L\text{-}L)]$ (L-L = 1,5-cyclooctadiene, 2,2′-bipyridine) give $[Pd(Fmes)Cl(L\text{-}L)]$ (L-L = COD, bipy) or $[Pd(Fmes)_2(bipy)]$. The structures of two complexes containing two Fmes ligands in *trans* and *cis* arrangement, *trans*-$[Pd(Fmes)_2(tht)_2]$ (**2**) and $[Pd(Fmes)_2(bipy)]$ (**6**), respectively, have been determined by X-ray diffraction. In spite of the severe steric congestion the complexes are four coordinated. Distortions due to the bulkiness of the *ortho* substituents and short Pd···F_3C-*ortho* distances are observed. The high degree of steric crowding is also responsible for slow rotation around the Pd−P bonds in the complex *trans*-$[Pd(Fmes)Cl(PPh_3)_2]$. $\Delta G^{\ddagger}$ associated with this motion is 12.8 kcal mol^{-1}, one of the highest values reported so far for rotation around M−PPh_3 bonds. Complexes **2** and **6** are redox inactive by cyclic voltammetry in the range −1.8 to +1.8 V.

Introduction

Fluoroaryl complexes of palladium or platinum, particularly C_6F_5 derivatives, have contributed greatly to the expansion of the chemistry of these metals. They have made possible the isolation and characterization of many new structural types of complexes in the solid state, facilitated studies in solution, and helped in the elucidation of reaction mechanisms.[1] These studies have been favored by the higher stability of fluoroaryl complexes compared to the analogous aryl derivatives, which has been explained by several factors, such as the greater electronegativity of the fluoroaryl ligand, which introduces a certain ionic character in the M−C bond, and some degree of M−fluoroaryl back-donation. A natural expansion of this chemistry is the use of other fluoroaryl ligands with different steric requirements, electronegativities, or symmetries.

The 2,4,6-tris(trifluoromethyl)phenyl (nonafluoromesityl or Fmes) group has been used recently as a ligand for main group metals,[2] such as Sn,[3] Pb,[4] Ga,[5] or In,[6] and induces unusual structural features such as the stabilization of low-coordinated complexes. Its coordination to Cu and group 12 metals has also been reported.[7] The stability of these complexes is attributed, in addition to the above mentioned factors common to fluoroaryls, to the steric bulk of the ligand and to the possibility of short metal−fluorine interactions involving the *ortho*-CF_3 groups. These properties should make the 2,4,6-tris(trifluoromethyl)phenyl group an interesting ligand also for transition metals, but so far there are only two reports on its coordination to middle transition metals: It is mentioned in a review that Herrmann's group has synthesized $Re(Fmes)O_3$,[2] and a recent communication has appeared reporting the syntheses of $Co(Fmes)_2$ and $Ni(Fmes)_2$,[8] although no X-ray structures have been reported.

Several points of interest can arise in complexes of the bulky Fmes ligand: (a) If the C_6F_5 derivatives (the fluoroaryl ligand most extensively used in palladium chemistry)[1a] show a certain degree of crowding, as revealed by many cases of restricted rotation around the M−C_6F_5 bonds,[9] the effects of crowding should be much

† E-mail: espinet@cpd.uva.es.
‡ E-mail: guy.orpen@bris.ac.uk.
⊗ Abstract published in *Advance ACS Abstracts,* March 15, 1996.

(1) (a) Usón, R.; Forniés, J. *Adv. Organomet. Chem.* **1988**, *28*, 219. (b) Maitlis, P. M.; Espinet, P.; Russell, M. J. H. In *Comprehensive Organometallic Chemistry*; Wilkinson, G., Stone, F. G. A., Abel, E. W., Eds.; Pergamon: Oxford, U.K., 1982; Chapter 38.4. (c) Hartley, F. R. *Ibid.*, Chapter 39.
(2) Edelmann, F. T. *Comments Inorg. Chem.* **1992**, *12*, 259.
(3) (a) Grützmacher, H.; Pritzkow, H.; Edelmann, F. T. *Organometallics* **1991**, *10*, 23. (b) Lay, U.; Pritzkow, H.; Grützmacher, H. *J. Chem. Soc., Chem. Commun.* **1992**, 260. (c) Vij, A.; Kirchmeier, R. L.; Willett, R. D.; Shreeve, J. M. *Inorg. Chem.* **1994**, *33*, 5456.
(4) Brooker, S.; Buijink, J.-K. Edelmann, F. T. *Organometallics* **1991**, *10*, 25.
(5) Schluter, R. D.; Isom, H. S.; Cowley, A. H.; Atwood, D. A.; Jones, R. A.; Olbrich, F.; Corbelin, S.; Lagow, R. J. *Organometallics* **1994**, *13*, 4058.
(6) Schluter, R. D.; Cowley, A. H.; Atwood, D. A.; Jones, R. A.; Bond, M. R.; Carrano, C. J. *J. Am. Chem. Soc.* **1993**, *115*, 2070.
(7) (a) Carr, G. E.; Chambers, R. D.; Holmes, T. F.; Parker, D. G. *J. Organomet. Chem.* **1987**, *325*, 13. (b) Brooker, S.; Bertel, N.; Stalke, D.; Noltenmeyer, M.; Roesky, H. W.; Sheldrick, G. M.; Edelmann, F. T. *Organometallics* **1992**, *11*, 192.
(8) Belay, M.; Edelmann, F. T. *J. Organomet. Chem.* **1994**, *479*, C21.
(9) (a) Casares, J. A.; Coco, S.; Espinet, P.; Lin, Y.-S. *Organometallics* **1995**, *14*, 3058. (b) Albéniz, A. C.; Cuevas, J. C.; Espinet, P.; de Mendoza, J.; Prados, P. *J. Organomet. Chem.* **1991**, *410*, 257. (c) Deacon, G. B.; Gatehouse, B. M.; Nelson-Reed, K. T. *Ibid.* **1989**, *359*, 267. (d) Crocker, C.; Goodfellow, R. J.; Gimeno, J.; Usón, R. *J. Chem. Soc., Dalton Trans.* **1977**, 1448. (e) Bennet, R. L.; Bruice, M. I.; Gardner, R. C. R. *Ibid.* **1973**, 2653.

0276-7333/96/2315-2019$12.00/0

Table 1. ^{19}F and ^{1}H NMR Data for the Fmes Group in the Complexes Described in This Work (Recorded at 283.6 and 300 MHz in $CDCl_3$ at Room Temperature Unless Otherwise Stated)

compd	*ortho*-CF_3[a]	*para*-CF_3[a]	H[a]
trans-Pd(Fmes)Cl(tht)$_2$, **1**	−60.1	−63.1	7.88
trans-Pd(Fmes)$_2$(tht)$_2$, **2**	−59.8	−63.1	7.90
trans-Pd(Fmes)Cl(PPh_3)$_2$, **3**	−58.6 (t, 5.6)	−63.3	7.08[b]
Pd(Fmes)Cl(COD), **4**	−57.0	−63.4	7.86
Pd(Fmes)Cl(bipy), **5**	−59.2	−63.0	7.92
Pd(Fmes)$_2$(bipy), **6**	−57.7	−63.1	7.79

[a] Singlets unless otherwise indicated (multiplicity, J_{PF} in Hz). [b] At −60 °C.

more important for Fmes. (b) M···F interactions are frequently found in Fmes complexes involving the fluorine atoms of the *ortho*-CF_3.[2] (c) The Fmes complexes should show a high degree of axial protection of the square-planar configuration, higher than those found for mesityl or *ortho*-$C_6H_4(CF_3)$ groups.[10] We report here the first complexes and X-ray structures containing the Fmes group attached to palladium(II) centers.

Results and Discussion

All the complexes containing Fmes described so far have been synthesized from its lithium derivative, Li(Fmes), which is easily produced by treating 1,3,5-tris(trifluoromethyl)benzene (FmesH) with LiBu and may be used *in situ*.[7a,11] The same method is used here, since attempted alternative methods were unsuccessful. Thus, the acidity of the hydrogens in FmesH is not sufficient to eliminate Hacac from [Pd(acac)$_2$] (no reaction after 5 h in refluxing toluene), whereas the reaction of [Pd(μ-Cl)(η^3-C_3H_5)]$_2$ with excess of FmesH in refluxing acetonitrile leads to deposition of metallic palladium. The presence of ancillary ligands seems important in obtaining well-defined (Fmes)palladium complexes, since the reaction of $PdCl_2$ with excess of Li(Fmes) for 24 h at 40 °C gave only a very small amount of an orange oil, which was a complex mixture of species by ^{19}F NMR. This is in contrast with the ready isolation of [Ni(Fmes)$_2$] and [Co(Fmes)$_2$], which have been described recently.[8] It is well-known that low-coordinate complexes are more easily obtained for smaller metals.

Therefore, the (Fmes)palladium(II) complexes described here were synthesized by treating Li(Fmes) with a variety of chloro complexes of palladium(II). Table 1 lists selected NMR data for the new complexes, and Table 2 gives the reaction conditions, products, and yields. An excess of Li(Fmes) (1:2 or 1:4) and moderate heating (40 °C) were used to promote the reaction with the bulky Fmes anion. These conditions usually induce decomposition and some deposition of metallic palladium but avoid the presence of unreacted chloro complexes, difficult to separate from the arylated products. In order to test the behavior of the ligand in different geometries, the following palladium(II) chloro complexes were chosen: *trans*-[$PdCl_2L_2$] (L = neutral monodentate ligand), to obtain mono- or bis-arylated *trans* complexes; [$PdCl_2$(L-L)] (L-L = neutral bidentate ligand), to isolate mono- or bis-arylated *cis* complexes. The products obtained from the reactions of [$PdCl_2L_2$] with an excess of Li(Fmes) depend on the size of L. When the bis-arylated complex can be formed, its formation is detected in even the 1/2 ratio reaction. This is the case for tht (tetrahydrothiophene) and bipy (2,2′-bipyridine) complexes, whereas for PPh_3 and COD (1,5-cyclooctadiene), which are more sterically demanding above and below the Pd(II) coordination plane, only the mono-arylated species are formed.

Table 2. Syntheses of New Complexes with Reactions Carried Out at 40 °C for 24 h Unless Otherwise Indicated

starting material	amt, mmol	molar ratio[a]	product(s) (yield, %)
trans-$PdCl_2$(tht)$_2$	1.00	1/2	**1** (67), **2** (4)
trans-$PdCl_2$(tht)$_2$	0.75	1/4	**2** (47)
trans-$PdCl_2$(PPh_3)$_2$	0.50	1/2	**3** (52)
$PdCl_2$(COD)	0.50	1/2	**4** (34)
$PdCl_2$(bipy)	1.50	1/2[b]	**5** (14), **6** (25)
$PdCl_2$(bipy)	0.50	1/4[c]	**6** (30)

[a] Chloro complex/LiFmes. [b] 5 h. [c] 7 h.

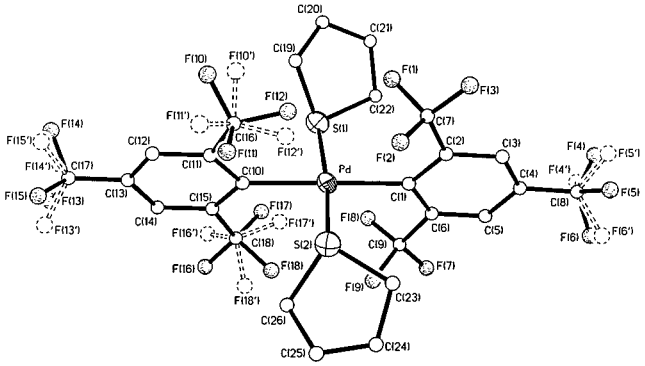

Figure 1. Molecular structure of **2** showing low-occupancy disordered fluorine atoms. All hydrogen atoms have been omitted for clarity.

(A) Arylation of *trans*-[$PdCl_2L_2$]. As shown in Table 2, the reaction of *trans*-[$PdCl_2$(tht)$_2$] with a 2-fold excess of Li(Fmes) leads to a 67% yield of orange *trans*-[Pd(Fmes)Cl(tht)$_2$], **1**, and a 4% yield of pale yellow *trans*-[Pd(Fmes)$_2$(tht)$_2$], **2**. The latter is selectively isolated in 47% yield when the reactant ratio used is 1/4. The presence of a chloro ligand in **1** is evident from its elemental analysis and in its IR spectrum which shows ν(Pd−Cl) at 290 cm^{-1}. The proposed *trans* geometry is confirmed by the equivalence of both tht ligands observed in the ^{1}H NMR spectrum (see Experimental Section). The *trans* geometry of **2** is not evident from its spectroscopic data but is proved by X-ray crystal structure analysis.

A perspective view of the molecular structure of **2** is given in Figure 1, and selected distances and angles are listed in Table 3. The crystal structure consists of isolated molecules separated by normal van der Waals contacts. Molecules of **2** show an approximately square-planar palladium(II) atom coordinated by two tht ligands and two Fmes ligands in *trans* positions. The two Pd−C bond lengths differ slightly (Pd−C(1) 2.083(5), Pd−C(10) 2.114(5) Å), while the Pd−S distances are essentially identical (Pd−S(1) 2.319(2), Pd−S(2) 2.311(2) Å). These Pd−C distances are somewhat longer than typical Pd−C

(10) (a) Ceder, R. M.; Cubillo, J.; Muller, G.; Rocamora, M.; Sales, J. *J. Organomet. Chem.* **1992**, *429*, 391. (b) Rieger, A. L.; Carpenter, G. B.; Rieger, P. H. *Organometallics* **1992**, *11*, 842. (c) Fallis, K. A.; Anderson, G. K.; Rath, N. P. *Organometallics* **1992**, *11*, 2423. (d) Klein, A.; Kaim, W. *Organometallics* **1995**, *14*, 1176.

(11) Scholz, M.; Roesky, H. N.; Stalke, D.; Keller, K.; Edelmann, F. T. *J. Organomet. Chem.* **1989**, *366*, 73. X-ray structure of [Et_2O·LiFmes]$_2$: Stalke, D.; Whitmire, K. H. *J. Chem. Soc., Chem. Commun.* **1990**, 833.

Table 3. Selected Bond Lengths (Å) and Angles (deg) for 2

Pd−C(1)	2.083(5)	Pd−C(10)	2.114(5)
Pd−S(2)	2.311(2)	Pd−S(1)	2.319(2)
C(1)−Pd−C(10)	178.9(2)	C(1)−Pd−S(2)	92.30(13)
C(10)−Pd−S(2)	87.81(13)	C(1)−Pd−S(1)	93.44(13)
C(10)−Pd−S(1)	86.54(13)	S(2)−Pd−S(1)	172.62(5)
C(2)−C(1)−C(6)	113.8(4)	C(2)−C(1)−Pd	124.3(4)
C(6)−C(1)−Pd	121.9(4)	C(3)−C(2)−C(1)	123.5(5)
C(3)−C(2)−C(7)	116.2(5)	C(1)−C(2)−C(7)	120.2(4)
C(4)−C(3)−C(2)	119.7(5)	C(5)−C(4)−C(3)	120.3(5)
C(5)−C(4)−C(8)	120.0(5)	C(3)−C(4)−C(8)	119.6(5)
C(4)−C(5)−C(6)	119.6(5)	C(5)−C(6)−C(1)	123.1(5)
C(5)−C(6)−C(9)	116.1(4)	C(1)−C(6)−C(9)	120.8(4)
F(3)−C(7)−C(2)	113.2(4)	F(1)−C(7)−C(2)	112.8(4)
F(2)−C(7)−C(2)	112.8(4)	F(4)−C(8)−C(4)	114.5(5)
F(5′)−C(8)−C(4)	117.8(11)	F(6′)−C(8)−C(4)	121.3(14)
F(6)−C(8)−C(4)	113.9(5)	F(4′)−C(8)−C(4)	101.5(14)
F(5)−C(8)−C(4)	113.2(5)	F(8)−C(9)−C(6)	112.9(5)
F(9)−C(9)−C(6)	112.6(5)	F(7)−C(9)−C(6)	112.6(5)
C(11)−C(10)−C(15)	113.1(4)	C(11)−C(10)−Pd	124.3(4)
C(15)−C(10)−Pd	122.5(4)	C(12)−C(11)−C(10)	123.2(5)
C(12)−C(11)−C(16)	113.2(5)	C(10)−C(11)−C(16)	123.6(4)
C(13)−C(12)−C(11)	120.5(5)	C(12)−C(13)−C(14)	119.8(5)
C(12)−C(13)−C(17)	120.0(5)	C(14)−C(13)−C(17)	120.2(5)
C(13)−C(14)−C(15)	119.7(5)	C(14)−C(15)−C(10)	123.6(5)
C(14)−C(15)−C(18)	113.6(5)	C(10)−C(15)−C(18)	122.8(4)
F(11′)−C(16)−C(11)	113.1(21)	F(10)−C(16)−C(11)	112.6(5)
F(12)−C(16)−C(11)	116.5(4)	F(12′)−C(16)−C(11)	117.9(24)
F(10′)−C(16)−C(11)	105.9(22)	F(11)−C(16)−C(11)	111.2(5)
F(15′)−C(17)−C(13)	116.3(9)	F(13)−C(17)−C(13)	116.4(5)
F(14′)−C(17)−C(13)	109.4(9)	F(14)−C(17)−C(13)	112.9(6)
F(13′)−C(17)−C(13)	112.5(8)	F(15)−C(17)−C(13)	113.4(5)
F(18′)−C(18)−C(15)	118.0(11)	F(17′)−C(18)−C(15)	115.6(12)
F(16)−C(18)−C(15)	115.3(5)	F(17)−C(18)−C(15)	114.5(5)
F(16′)−C(18)−C(15)	108.2(10)	F(18)−C(18)−C(15)	112.9(4)

lengths in Pd−C_6F_5 complexes [which average 2.025(6) Å (sample standard deviation 0.036 Å) in 33 examples from the Cambridge Structural Database]. The Pd−S distances are in the usual range for Pd(II)−tht complexes [which average 2.321(5) Å (sample standard deviation 0.012 Å) in 7 examples from the Cambridge Structural Database]. The coordination angles at palladium are near the square planar ideal, but the *cis* angles involving the shorter Pd−C bond are larger than those for the other (C(1)−Pd−S(1) 92.30(13), C(1)−Pd−S(2) 93.44(13), C(10)−Pd−S(1) 86.54(13), C(10)−Pd−S(2) 87.81(13)°). The palladium atom lies somewhat out of the mean plane of the aryl groups (by 0.079 and 0.105 Å for rings C(1−6) and C(10−15), respectively; *cf.* mean carbon atom displacements of 0.006 and 0.005 Å).

The geometry of the aryl ligands is similar to that observed in other complexes of the Fmes ligand which do not contain ancillary ligands,[3−6,7b] showing that the presence of the two tht groups does not substantially affect the geometry of the fluoroaryl ligand. Thus the C−C−C angle at the *ipso* carbon is significantly less than 120° (*ca.* 113° in **2**) and those at the *ortho* carbons rather larger than 120° (*ca.* 123° in **2**) as a result of the electronic effects of the electropositive metal and electronegative CF_3 substituents at these positions.[12] The *ortho*-CF_3 groups lie close to the axial sites above and below the palladium coordination plane, with the shortest Pd···F distances being Pd···F(12) 2.897, Pd···F(12′) 2.982, and Pd···F(17′) 2.936 Å. The C−C−CF_3 angles show systematic distortions with the C_{ipso}−C_{ortho}−CF_3 angles being larger than the C_{meta}−C_{ortho}−CF_3 angles by 4 or 10° (*ca.* 120 *vs* 116° for one of the Fmes ligands and *ca.* 123 *vs* 113° for the other Fmes group; see Table 3). The lengthening of the Pd−C bond, these angular distortions, and the displacement of the metal from the C_6 plane are all consistent with a high degree of steric crowding resulting from the presence of the CF_3 *ortho* substituents.

It is interesting to compare these short Pd···F distances with other cases of short M···X "contacts". For this we use the parameter ρ, defined as experimental distances/sum of the covalent radii, $d/[r(M) + r(X)]$,[13] and take $r(F) = 0.64$ Å,[14] as used in the reference (a shorter $r(F)$ value is given in more modern texts,[15] which would make all ρ values where F is involved about 0.05 larger). In complex **2**, $\rho = 1.51$ for the shortest Pd···F(12) distance (2.897 Å), this value being somewhat larger than those reported for the *o*-F···Ag contacts in a large series of binuclear C_6F_5Pt−Ag complexes, which are in the range 1.31−1.48.[13] There are no previous reports on Pd···F contacts, but the shortest Pd···O contact reported (2.651 Å) gives $\rho = 1.32$.[16] Larger distances (about 3 Å), but smaller ρ values (1.28 for the shortest distance), are found for Pd···S contacts.[17] Other fluoromesityl complexes show M···F contacts in the ranges $\rho = 1.31-1.39$ for Sn(II),[3a] $\rho = 1.28-1.36$ for Pb(II),[4] $\rho = 1.38-1.49$ for Zn(II), $\rho = 1.36-1.43$ for Cd(II), $\rho = 1.50-1.58$ for Hg(II),[7b] $\rho = 1.41-1.51$ for Ga(III),[5] and $\rho = 1.27-1.31$ for In(III).[6] Whereas the presence of bonding interactions has been concluded in all these cases of short contacts in which the metal atoms are coordinatively unsaturated, we feel that in **2** an extra covalent interaction between a soft 16e palladium center and a hard fluorocarbon fluorine atom is unlikely. Indeed, the geometrical distortions observed in the complex seem to occur in order to allow for a larger nonbonding Pd···F distance, as discussed below.

The fluorine atoms in the *ortho*-CF_3 group are all equivalent when the complex is in solution, giving rise to one singlet in the ^{19}F NMR at room temperature (Table 1). Low-temperature NMR spectra were recorded to see whether the rotation of the CF_3 group might be slowed down due to the high steric crowding. However, the spectra remain invariant even at −90 °C in CD_2Cl_2 solution.

A different situation is found in *trans*-[Pd(Fmes)Cl-$(PPh_3)_2$], **3**. This complex is obtained in a 52% yield as a white solid from the 1:2 reaction of *trans*-[$PdCl_2$-$(PPh_3)_2$] and Li(Fmes). As indicated before, no bisarylated species are detected in this reaction. The coordination of the chlorine atom in **3** is confirmed by

(12) (a) Domenicano, A.; Vaciago, A.; Coulson, C. A. *Acta Crystallogr., Sect. B* **1975**, *31*, 221. (b) Domenicano, A.; Murray-Rust, P.; Vaciago, A. *Acta Crystallogr., Sect. B* **1983**, *39*, 457 and references therein. (c) Norrestam, R.; Schepper, L. *Acta Chem. Scand., Ser. A.* **1981**, *35*, 91. (d) Domenicano, A.; Mazzeo, P.; Vaciago, A. *Tetrahedron Lett.* **1976**, 1029.

(13) (a) Usón, R.; Forniés, J.; Tomás, M. *J. Organomet. Chem.* **1988**, *358*, 525. (b) Usón, R.; Forniés, J. *Inorg. Chim. Acta* **1992**, *198*−200, 165.

(14) Pauling, L. *The Nature of the Chemical Bond*, 3rd ed.; Cornell University Press: Ithaca, NY, 1960; p 403.

(15) Emsley, J. *The Elements*, 2nd ed.; Oxford University Press: Oxford, U.K., 1991.

(16) Dunbar, K. R.; Sun, J.-S. *J. Chem. Soc., Chem. Commun.* **1994**, 2387.

(17) (a) Blake, A. J.; Gould, R. O.; Lavery, A. J.; Schröder, M. *Angew. Chem., Int. Ed. Engl.* **1986**, *25*, 274. (b) Wieghardt, K.; Küppers, H.-J.; Raabe, E.; Krüger, C. *Ibid.* **1986**, *25*, 1101. (c) Blake, A. J.; Holder, A. J.; Hyde, T. I.; Roberts, Y. V.; Lavery, A. J.; Schröder, M. *J. Organomet. Chem.* **1987**, *323*, 261. (d) Grant, G. T.; Sanders, K. A.; Setzer, W. N.; VanDerveer, D. G. *Inorg. Chem.* **1991**, *30*, 4053. (e) de Groot, B.; Hanan, G. S.; Loeb, S. J. *Inorg. Chem.* **1991**, *30*, 4644. (f) Blake, A. J.; Crofts, R. D.; de Groot, B.; Schröder, M. *J. Chem. Soc., Dalton Trans.* **1993**, 485.

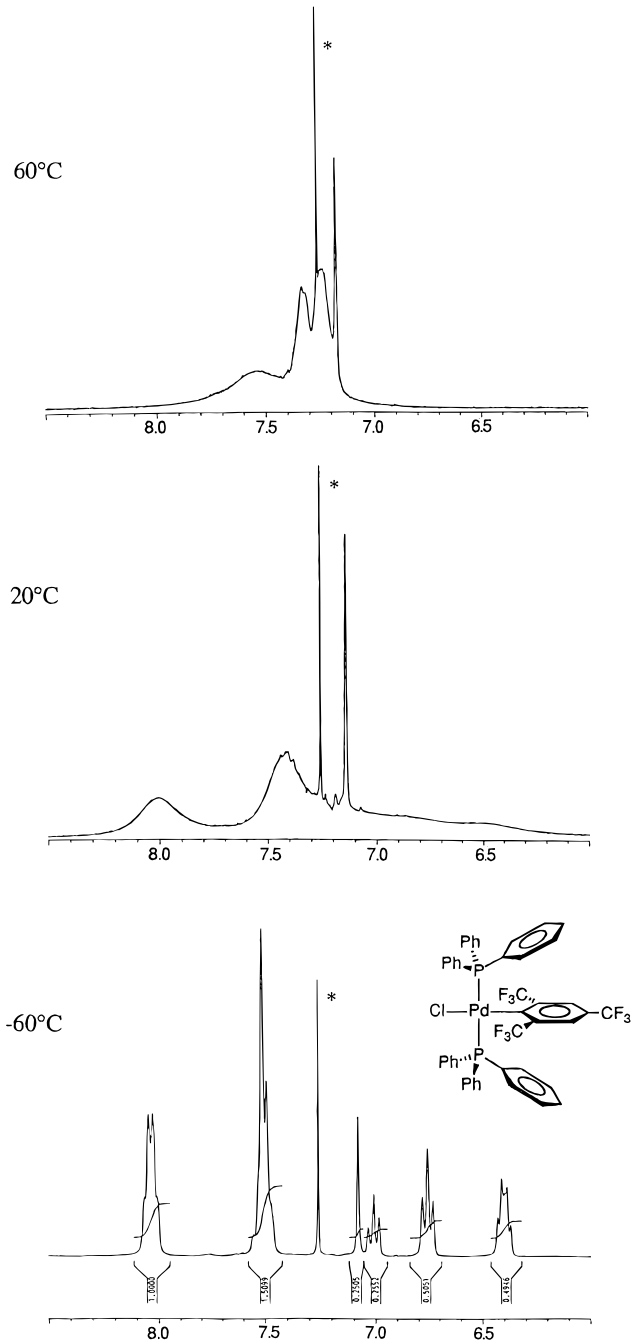

Figure 2. ^{1}H NMR spectra at different temperatures of **3** (* indicates $CDCl_3$, 300 MHz).

IR spectroscopy (ν(Pd−Cl) at 302 cm^{-1}), and the *trans* geometry is demonstrated by its $^{31}P\{^1H\}$ NMR spectrum, which shows only one signal (δ 21.3 ppm, septet, J_{PF} 5.6 Hz) showing the equivalence of the PPh_3 ligands. The ^{19}F NMR spectrum shows one triplet for the *ortho* CF_3 coupled to two equivalent P atoms, consistent with this structure assignment.

The ^{19}F and $^{31}P\{^1H\}$ NMR spectra remain invariant from −60 °C to room temperature. However, the ^{1}H NMR spectrum of **3** at room temperature shows broad signals for the aromatic hydrogens of the PPh_3 ligand which do not preclude the observation of the Fmes hydrogens as a clean singlet (Figure 2). The spectrum changes on heating at 60 °C toward a pattern more typical of PPh_3 hydrogens (although still somewhat broad). On cooling of the sample at −60 °C the spectrum shows (see Figure 2 and Experimental Section) one phenyl ring to differ from the other two, the signals of the first appearing at higher field than normal, whereas those of the other two have normal chemical shifts. The hydrogen signals of the shielded phenyl group follow the sequence (δ in parentheses): *ortho*-H (6.4) > *meta*-H (6.8) > *para*-H (7.0). Furthermore, a marked shielding is also found for the signal due to the two hydrogens of the Fmes ligand (δ = 7.08 in **3**, *vs* 7.79−7.91 ppm for the rest of complexes herein described; see Table 1). These observations may be interpreted by postulating that the rotation around the Pd−P bonds has been arrested at low temperature in the arrangement shown in Figure 2, where the hydrogen atoms of the fluoroaryl ligand and those of one of the phenyl groups of each phosphine are subjected to high shielding anisotropy due to interaction with the aryl rings.

Restricted rotation around M−PR_3 bonds has been reported previously by several authors, associated with stereochemically crowded systems.[18] In **3**, the activation free energy measured at 208.8 K by spin saturation transfer experiments (see Experimental Section) was $\Delta G^{\ddagger}$ = 12.8 kcal mol^{-1}, which is among the highest values reported so far for a barrier to rotation around a M−PPh_3 bond. As $\Delta S^{\ddagger}$ for the rotation process has been shown to be very close to zero, then $\Delta G^{\ddagger} \approx \Delta H^{\ddagger}$, and a comparison with other $\Delta G^{\ddagger}$ values measured at different temperatures can be made.[18b] The $\Delta G^{\ddagger}$ values reported for rotation of the bulky P^{t}Bu$_2$R (R = H, CH_3, Ph) in [MX(CO)(P^{t}Bu$_2$R)$_2$] (X = Cl, Br, I; M = Rh, Ir) are in the range 12−16 kcal mol^{-1},[18e−f] but the values reported for PPh_3 complexes lie in the range 8−10 kcal mol^{-1}.[18a−d] The highest value in the literature for PPh_3 square-planar complexes has been reported recently within the series *cis*-[PtX_2(Me$_2$phen)(PPh_3)] (Me$_2$phen = monodentate 2,9-dimethyl-1,10-phenanthroline) were $\Delta G^{\ddagger}$ = 10.2, 10.8, and 11.8 kcal mol^{-1} for X = Cl, Br, and I, respectively. The high-energy barrier to rotation in this case has been attributed to a stacking interaction between one phenyl ring of PPh_3 and the aromatic system of the Me$_2$phen ligand acting as a type of intramolecular brake, rather than to steric effects.[18a]

In order to ascertain whether the barrier to rotation in our case was related to stacking interactions or to steric effects, the complex *trans*-[Pd(C_6F_5)Cl(PPh_3)$_2$] was studied. Only a slight broadening was observed in the ^{1}H and $^{13}C\{^1H\}$ NMR at −90 °C in CD_2Cl_2, which means that $\Delta G^{\ddagger}$ should be noticeably lower than 8 kcal mol^{-1}. Consequently the barrier to rotation observed in **3** must be attributed mostly to steric effects.

As stated above, the size of the ancillary ligands greatly influences the products obtained in the syntheses. This was confirmed by additional reactions of other *trans*-[$PdCl_2$(PR_3)$_2$] complexes with Li(Fmes), which showed a clear dependence on the cone angle of the phosphine. Thus, the reaction of [$PdCl_2$(PMe_3)$_2$] with

(18) (a) Fanizzi, F. P.; Lanfranchi, N.; Natile, G.; Tiripicchio, A. *Inorg. Chem.* **1994**, *33*, 3331. (b) Davies, S. G.; Derome, A. E.; McNally, J. P. *J. Am. Chem. Soc.* **1991**, *113*, 2854 and references therein. (c) Chudek, J. A.; Hunter, G.; MacKay, R. L.; Kremminger, P.; Schlögl, K.; Weissensteiner, W. *J. Chem. Soc., Dalton Trans.* **1990**, 2001. (d) Hunter, G.; Weakley, T. J. R.; Weissensteiner, W. *Ibid.* **1987**, 1545 and references therein. (e) DiMeglio, C. M.; Luck, L. A.; Rithner, C. D.; Rheingold, A. L.; Elcesser, W. L.; Hubbard, J. L.; Bushweller, C. H. *J. Phys. Chem.* **1990**, *94*, 6255 and references therein. (f) Bushweller, C. H.; Rithner, C. D.; Butcher, D. J. *Inorg. Chem.* **1986**, *25*, 1610. (g) Jones, W. D.; Feher, F. J. *Inorg. Chem.* **1984**, *23*, 2376. (h) Selnau, H. E.; Merola, J. S. *Organometallics* **1993**, *12*, 1583.

4 equiv of Li(Fmes) led to a complex mixture which could not be separated by column chromatography nor fully identified by its NMR spectra. A mixture of *cis* and *trans* isomers can be expected from the *cis*−*trans* equilibrium observed in the solutions of the starting material.[19] Thus two (*cis* and *trans*) mono-arylated and two bis-arylated species are possible, in addition to dimeric species of the type $[Pd_2(\mu\text{-}Cl)_2(Fmes)_2(PMe_3)_2]$ (two possible isomers), or even more highly arylated anionic species. Since the NMR spectra of the crude product revealed the presence of more than four complexes, it seems very likely that bis-arylated complexes are present in the mixture. It appears then that the small cone angle of PMe_3 (118°)[20] allows bis-arylated complexes to be formed, whereas the bulkier PPh_3 (145°) stops the reaction at the mono-arylated complex. Furthermore, *trans*-$[PdCl_2(PCy_3)_2]$ (Cy = cyclohexyl) does not react with Li(Fmes) and the starting material is recovered unchanged. In this case, the phosphine is presumably too bulky (cone angle 170°) and prevents coordination of Fmes.

(B) Arylation of $[PdCl_2(L\text{-}L)]$. The reaction of $[PdCl_2(COD)]$ with Li(Fmes) using a 1:2 molar ratio gives a 34% yield of [Pd(Fmes)Cl(COD)], **4**, as a pale yellow crystalline solid. This stoichiometry is supported by the observation of ν(Pd−Cl) at 323 cm^{-1} in the IR spectrum, the presence of signals due to two nonequivalent halves of the COD ligand in the ^1H NMR spectrum, and the analytical data. The bis-arylated product, or species resulting from insertion reactions of COD in the Pd−$C_6H_2(CF_3)_3$ bond (as found for $[Pd(C_6F_5)Cl(COD)]$),[21] were not detected in this reaction. The bis-arylated product is probably disfavored due to severe steric effects above and below the coordination plane. In effect, a *cis*-bis-arylated complex is cleanly isolated when the chelating ligand is confined to the coordination plane, e.g. when using bipy instead of COD. Thus reaction of $[PdCl_2(bipy)]$ with a 2- fold excess of Li(Fmes) yields 14% of [Pd(Fmes)Cl(bipy)], **5**, as a yellow solid, and 26% of $[Pd(Fmes)_2(bipy)]$, **6**, as an off-white solid; using a 1:4 ratio and a longer reaction time only complex **6** is formed in 30% yield.

The IR spectrum of **5** shows a Pd−Cl absorption at 340 cm^{-1}, whereas the ^1H NMR spectrum reveals the presence of an asymmetric bipy, as the two ligands *trans* to the nitrogen atoms are different. One H^6 of the bipy ligand, *cis* to the chloro ligand, appears clearly shielded.[22] The analytical data for **6** support the presence of two Fmes ligands in the complex, and the ^1H NMR spectrum suggests that the molecule is symmetrical with equivalent Fmes groups and the two halves of the bipy ligand equivalent. The presence of a *cis*-bis(Fmes) moiety in **6** prompted us to determine its solid structure by X-ray diffraction, as there are no previous reports of complexes containing two Fmes ligand with this geometry and also as to provide a comparison with the structure of **2**, which contains a *trans*-bis(Fmes) moiety.

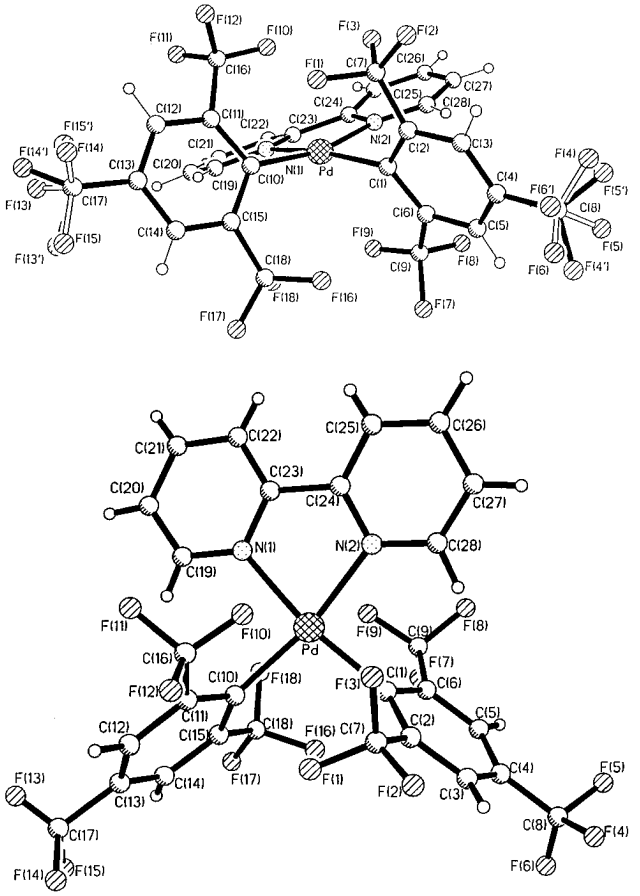

Figure 3. Two perspective views of the molecular structure of **6**: (a) View showing low-occupancy disordered fluorine atoms; (b) view with minor component disordered fluorine atoms omitted for clarity.

Figure 3 shows two different perspective views of the molecular structure of **6**, and selected distances and angles are listed in Table 4. The crystal consists of isolated molecules separated by normal van der Waals contacts. The two Fmes ligands are coordinated in a *cis* arrangement, and the two nitrogen atoms of the 2,2′-bipyridyl ligand occupy the other two coordination sites. The Pd−C distances are very similar (Pd−C(1) 2.032(3), Pd−C(10) 2.023(3) Å) and similar to typical Pd−C lengths in Pd−C_6F_5 complexes as noted above. The Pd−N distances (Pd−N(1) 2.110(2), Pd−N(2) 2.103(3) Å) are normal and slightly shorter than those found in the acyl complex $[Pd(CO_2Me)_2bipy]$.[23]

The expected square-planar geometry is severely distorted. Thus, the N(1)−Pd−N(2) angle is smaller than 90° (78.83(9)°); this is normal for a small-bite chelating ligand such as bipy and comparable to the angle found in $[Pd(CO_2Me)_2bipy]$ (77.6(3)°). The *cis* angle involving the carbon atoms of the Fmes ligands is larger than 90° (C(1)−Pd−C(10) 96.88(10)°). This is in contrast with the C−Pd−C angle found in $[Pd(CO_2Me)_2bipy]$ (87.0(5)°); presumably the opening of this angle in **6** is imposed by steric constraints. With respect to the plane described by the Pd, N(1), and N(2) atoms, the 2-pyridyl groups are below (left in Figure 3a) and above (right in Figure 3a) this plane (N−C−C−N torsion angle = 13.1(2)°), whereas the Pd−C bonds in *cis* positions are respectively bent above and below, as is

(19) Goodfellow, R. F.; Evans, J. G.; Goggin, P. L.; Duddell, D. A. *J. Chem. Soc. A* **1968**, 1604.
(20) McAuliffe, C. A. In *Comprehensive Coordination Chemistry*; Wilkinson, G., Gillard, R. D., McCleverty, J. A., Eds.; Pergamon: Oxford, U.K., 1987; Vol. 2, pp 1012−1029.
(21) Albéniz, A. C.; Espinet, P.; Jeannin, Y.; Philoche-Levisalles, M.; Mann, B. E. *J. Am. Chem. Soc.* **1990**, *112*, 6594.
(22) (a) Byers, P. K.; Canty, A. J. *Organometallics* **1990**, *9*, 210. (b) Rülke, R. E.; Ernsting, J. M.; Spek, A. L.; Elsevier, C. J.; van Leeuwen, P. W. N. M.; Vrieze, K. *Inorg. Chem.* **1993**, *32*, 5769.
(23) Smith, G. D.; Hanson, B. E.; Merola, J. S.; Waller, F. J. *Organometallics* **1993**, *12*, 568.

Table 4. Selected Bond Lengths (Å) and Angles (deg) for 6

Pd−C(1)	2.032(3)	Pd−C(10)	2.023(3)
Pd−N(1)	2.110(2)	Pd−N(2)	2.103(2)
C(1)−Pd−C(10)	96.88(10)	N(2)−Pd−N(1)	78.83(9)
C(1)−Pd−N(1)	166.57(10)	C(10)−Pd−N(1)	92.38(10)
C(1)−Pd−N(2)	93.82(10)	C(10)−Pd−N(2)	165.75(10)
C(2)−C(1)−Pd	127.1(2)	C(11)−C(10)−Pd	118.6(2)
C(6)−C(1)−Pd	119.3(2)	C(15)−C(10)−Pd	126.9(2)
C(2)−C(1)−C(6)	113.3(2)	C(11)−C(10)−C(15)	114.0(2)
C(1)−C(2)−C(3)	123.0(3)	C(10)−C(11)−C(12)	122.9(3)
C(1)−C(2)−C(7)	120.8(3)	C(10)−C(11)−C(16)	125.6(2)
C(3)−C(2)−C(7)	116.1(3)	C(12)−C(11)−C(16)	111.4(3)
C(2)−C(3)−C(4)	121.0(3)	C(11)−C(12)−C(13)	120.3(3)
C(3)−C(4)−C(5)	118.3(3)	C(12)−C(13)−C(14)	119.4(3)
C(3)−C(4)−C(8)	121.2(3)	C(12)−C(13)−C(17)	118.7(3)
C(5)−C(4)−C(8)	120.5(3)	C(14)−C(13)−C(17)	121.9(3)
C(4)−C(5)−C(6)	121.2(3)	C(13)−C(14)−C(15)	120.2(3)
C(5)−C(6)−C(1)	123.1(3)	C(14)−C(15)−C(10)	123.0(3)
C(5)−C(6)−C(9)	111.3(3)	C(14)−C(15)−C(18)	115.9(2)
C(1)−C(6)−C(9)	125.6(2)	C(10)−C(15)−C(18)	121.0(2)
C(2)−C(7)−F(1)	114.3(3)	C(11)−C(16)−F(10)	117.4(2)
C(2)−C(7)−F(2)	112.8(3)	C(11)−C(16)−F(11)	109.8(3)
C(2)−C(7)−F(3)	111.9(3)	C(11)−C(16)−F(12)	111.9(3)
C(4)−C(8)−F(4)	112.8(5)	C(13)−C(17)−F(13)	107.3(9)
C(4)−C(8)−F(4′)	111.4(5)	C(13)−C(17)−F(13′)	114.0(6)
C(4)−C(8)−F(5)	111.4(4)	C(13)−C(17)−F(14)	112.7(5)
C(4)−C(8)−F(5′)	111.7(6)	C(13)−C(17)−F(14′)	114.8(5)
C(4)−C(8)−F(6)	116.6(5)	C(13)−C(17)−F(15)	112.9(5)
C(4)−C(8)−F(6′)	110.4(5)	C(13)−C(17)−F(15′)	112.0(5)
C(6)−C(9)−F(7)	110.7(3)	C(15)−C(18)−F(16)	113.9(2)
C(6)−C(9)−F(8)	110.2(2)	C(15)−C(18)−F(17)	113.2(3)
C(6)−C(9)−F(9)	117.6(2)	C(15)−C(18)−F(18)	112.1(2)

clearly shown in Figure 3a, leading to a marked distortion of the square-planar coordination toward tetrahedral.

The fluoroaryl groups are not perpendicular to the coordination plane, as is common in all aryl derivatives, but tilt in the same sense by 70.4 and 70.2°. Similar behavior has been also observed in the closely related structure of [PtMes$_2$(bipy)].[24] All these distortions may be attributed to the high steric crowding in the complex and help to keep the *ortho*-CF_3 of the two Fmes ligands apart from each other. Only one F atom of each Fmes group comes close to the Pd atom leading to short contacts Pd···F(9) 2.788 Å (ρ = 1.45) and Pd···F(10) 2.766 Å (ρ = 1.44), shorter than those found in **2** (see above).

Finally, the geometry of the Fmes ligands in **6** is very similar to that of **2** and of other Fmes compounds reported.[3−6,7b] The C−C−C angle at the *ipso*-carbon is significantly less than 120° (C(2)−C(1)−C(6) 113.3(2), C(11)−C(10)−C(15) 114.0(2)°), and those at the *ortho*−carbons are larger than 120° (*ca.* 123°), as reported in other cases.[12] The C−C−CF_3 angles show also systematic distortions, with the C_{ipso}−C_{ortho}−CF_3 angles being always larger than the C_{meta}−C_{ortho}−CF_3 angles. In contrast to **2**, the two Fmes ligands in **6** are almost equivalent, each showing two very different *ortho*-CF_3 substituents: one pseudo-apical (C(9)F_3 and C(16)F_3) and one pseudo-equatorial (C(7)F_3 and C(18)F_3) with respect to the metal center. For the pseudo-apical CF_3 groups the C_{ipso}−C_{ortho}−CF_3 and C_{meta}−C_{ortho}−CF_3 angles differ by *ca.* 14.5° (125.6° for both *vs ca.* 111°; see Table 4), whereas for the pseudo-equatorial *ortho*-CF_3 groups the corresponding difference is only about 4.5° (*ca.* 120.5° *vs ca.* 116°; see Table 4). Therefore these geometrical distortions seem to be forced in order to allow for a larger nonbonding Pd···F distance as discussed below.

(24) Klein, A.; Hausen, H.-D.; Kaim, W. J. *J. Organomet. Chem.* **1992**, *440*, 207.
(25) Bondi, A. *J. Chem. Phys.* **1964**, *68*, 441 and references therein.

Chart 1. Schematic Representations of the Fragments of 2 Directly Involved in the Crowding around the Pd Center, with Relevant Distances and Angles*

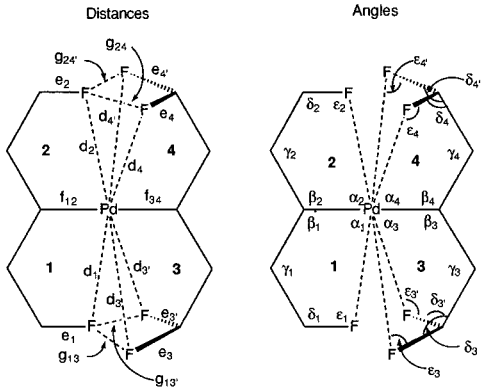

	1[F(12)]	2[F(18)]	3[F(1)]	3'[F(2)]	4[F(8)]	4'[F(9)]
d	2.897	3.135	3.234	3.288	3.212	3.225
e	1.313	1.331	1.335	1.342	1.318	1.328
f	2.114		2.083			
g_1 or g_2			2.783	2.781	3.180	2.677
α	68.2	64.9	63.7	63.5	64.7	64.7
β	124.3	122.5	124.3		121.9	
γ	123.6	122.8	120.2		120.8	
δ	116.5	112.9	112.8	112.8	112.6	112.9
ε	104.6	90.1	83.8	81.5	82.8	82.2

* Distances and angles are given for the major conformations of the CF_3 groups only.

As in complex **2**, the *ortho*-CF_3 groups in **6** are equivalent when the complex is in solution and give rise to one singlet in the ^{19}F NMR at room temperature (Table 1). Since the bulk of the Fmes ligands excludes their free rotation around the Pd−C bond (hindered also in *cis* complexes with smaller aryls),[9] the equivalence must be achieved by a concerted tilting of the two Fmes ligands, so that the average situation corresponds to the Fmes coordinated perpendicular to the palladium square plane. This movement cannot be completely stopped even at −90 °C (CD_2Cl_2 solution), but the ^{19}F NMR spectrum at this temperature shows broadening of the signal of the *ortho*-CF_3 groups, whereas that of the *para*-CF_3 remains sharp.

Comparison of the Structures of 2 and 6. Schematic representations of the fragments of **2** and **6** more directly involved in the crowding around the Pd center, with relevant angles and distances, are shown in Charts 1 and 2, respectively. Two different kinds of steric hindrance occur in the bis(Fmes) complexes: competition of two CF_3 groups for the space close to the *z* axis above and below the metal coordination plane (*xy*); the short distances between the F atoms and the Pd atom imposed by the bulkiness of the *ortho* substituents.

The two complexes studied adopt different strategies to minimize the interactions between F atoms of the two aryl rings, some of which are in the lowest limit expected for F···F nonbonding contacts (the literature F···F van der Waals distance is 2.8−3.00 Å).[25] In the *trans* complex **2** each Fmes group has its two *ortho*-CF_3 groups

Chart 2. Schematic Representations of the Fragments of 6 More Directly Involved in the Crowding around the Pd Center, with Relevant Distances and Angles*

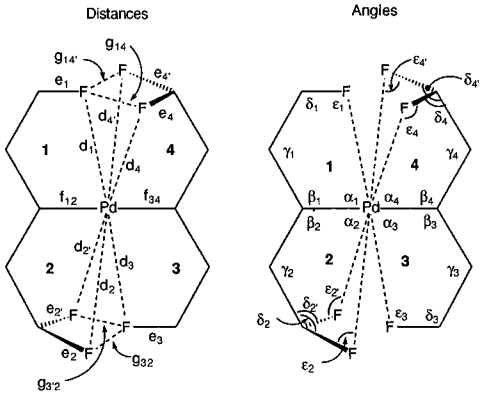

	1[F(10)]	2[F(16)]	2'[F(18)]	3[F(9)]	4[F(1)]	4'[F(3)]
d	2.766	3.473	3.213	2.788	3.508	3.220
e	1.308	1.330	1.338	1.307	1.322	1.341
f	2.033			2.032		
g_3 or g_1		2.675	3.148		3.190	2.696
α	74.2	61.1	63.8	73.5	60.6	63.2
β	118.6	126.9		119.3	127.1	
γ	125.6	121.0		125.6	120.8	
δ	117.4	113.9	112.1	117.6	114.3	111.9
ε	102.5	76.3	86.9	103.0	75.5	87.0

* Distances and angles are given for the major conformations of the CF_3 groups only.

similarly disposed. The Fmes at the right in Chart 1 has two "staggered" CF_3 groups each with two F atoms at distances to Pd (*d*, average 3.240 Å) larger than the sum of van der Waals radii (3.10−3.20 Å) and making smaller C_{ipso}−Pd···F angles (α, average 64.2°); this ligand shows the shorter C_{ipso}−Pd distance (*f*) and smaller C_{ipso}−C_{ortho}−CF_3 angles (γ). The Fmes at the left in Chart 1 has two CF_3 groups with fluorine atoms eclipsed relative to the palladium center with one F atom at a short distance (d_1, d_2, 2.897, 3.135 Å) and making larger C_{ipso}−Pd···F angles (α_1, α_2, 68.2, 64.9°). This Fmes ligand shows the larger C_{ipso}-Pd distance (*f*) and larger C_{ipso}−C_{ortho}−CF_3 angles (γ). These differences suggest that the distances and angles in the Fmes with the eclipsed CF_3 groups are somewhat distorted in order to keep F(12) and F(18) as far from Pd as possible.

In the *cis* complex **6** each Fmes group has one *ortho*-CF_3 group in a staggered orientation with respect to the metal (that in the pseudo-apical site; see above) and one eclipsed (pseudo-equatorial), as is clearly seen in Figure 3b. As depicted in Chart 2, the two staggered CF_3 groups, one in each in one Fmes group, have two F atoms with Pd···F distance larger than the sum of van der Waals radii (all Pd···F > 3.2 Å) and making smaller C_{ipso}−Pd···F angles (α, average 62.2°) and smaller C_{ipso}−C_{ortho}−CF_3 angles (γ). The two eclipsed CF_3 groups have one F atom with a shorter Pd···F distance (d_1, d_3, 2.766, 2.788 Å, noticeably shorter than in **2**) and making larger C_{ipso}−Pd···F angles (α_1, α_3, 74.2, 73.5°, noticeably larger than in **2**); they also have larger C_{ipso}−C_{ortho}−CF_3 (γ) and C_{ortho}−C−F (δ) angles. These differences are all more marked than in the *trans* complex and strongly suggest a direct relationship in the sense that short Pd···F distances are associated with larger C_{ipso}−Pd···F and C_{ipso}−C_{ortho}−CF_3 (γ) and C_{ortho}−C−F (δ) angles, which distortions allow for larger eclipsed Pd···F distances.

Electrochemical Studies on 2 and 6. Electrochemical studies were carried out on complexes **2** and **6** in dichloromethane as solvent in the range −1.8 to +1.8 V to check whether oxidation accompanied by F coordination might occur. Both complexes turned out to be electrochemically inert in the range of potentials studied, and this supports the view that the short Pd···F distances observed do not imply bonding interaction.

Conclusions

The coordination of two bulky 2,4,6-tris(trifluoromethyl)phenyl groups to palladium(II) does not lead to the formation of coordinatively unsaturated species but to very crowded basically square-planar complexes, whether in the *cis* or in the *trans* isomer. However, these bis-arylated complexes are not accessible for ancillary ligands of medium size. The crowding in the bis-arylated complexes produces very short nonbonding Pd···F and F···F contacts.

The crowding seems to be the main reason for the severe restriction observed to the rotation of the PPh_3 ligands around the P-Pd bonds in *trans*-[Pd(Fmes)Cl-$(PPh_3)_2$], since such restriction is not observed in the electronically comparable *trans*-[Pd(C_6F_5)Cl(PPh_3)$_2$].

Experimental Section

General Comments. All reactions were carried out under an atmosphere of dry dinitrogen. Diethyl ether was distilled under nitrogen from sodium/benzophenone ketyl prior to use, and the rest of solvents were purified according to standard procedures.[26] The complexes *trans*-[$PdCl_2$(tht)$_2$], *trans*-[$PdCl_2$-$(PPh_3)_2$], [$PdCl_2$(COD)], [$PdCl_2$(bipy)], and *trans*-[Pd(C_6F_5)Cl-$(PPh_3)_2$] were prepared according to literature procedures.[27] 1,3,5-$C_6H_3(CF_3)_3$ (FmesH) was purchased from Fluorochem and used as received. Li(Fmes) was prepared as described in the literature,[7a,11a] using a *ca.* 0.6 M solution of FmesH in hexane, and used immediately *in situ* without further purification.

Infrared spectra were recorded in a Perkin-Elmer 883 apparatus as Nujol mulls between polystyrene films from 4000 to 200 cm^{-1}. NMR spectra were recorded on Bruker AC-300 or ARX-300 instruments at room temperature unless otherwise stated. NMR spectra are referred to TMS, 85% aqueous H_3PO_4, and $CFCl_3$. ^{19}F NMR data for the new compounds are collected in Table 2. Elemental analyses were performed on a Perkin-Elmer 2400B microanalyzer. Cyclic voltammetry experiments were carried out using a EG&G Model Versastat 253 in conjunction with a three-electrode cell under experimental conditions described elsewhere.[28]

General Method for the Preparation of New Complexes. Molar ratios of the reactants, products, and yields are collected in Table 2. The solid chloro complex was added under nitrogen to a solution of Li(Fmes) in Et_2O (10 mL/mmol of lithium derivative). The reaction mixture was maintained

(26) Perrin, D. D.; Armarego, W. L. F. *Purification of Laboratory Chemicals*, 3rd ed.; Pergamon Press: Oxford, U.K., 1988.

(27) (a) Usón, R.; Forniés, J.; Martínez, F.; Tomás, M. *J. Chem. Soc., Dalton Trans.* **1980**, 888. (b) Jenkins, J. M.; Verkade, J. G. *Inorg. Synth.* **1968**, *11*, 108. (c) Drew, D.; Doyle, J. R. *Ibid.* **1990**, *28*, 348. (d) Wimmer, F. L.; Wimmer, S.; Castan, P. *Ibid.* **1992**, *29*, 185. (e) Usón, R.; Royo, P.; Forniés, J.; Martínez, F. *J. Organomet. Chem.* **1975**, *90*, 367.

(28) Espinet, P.; García-Herbosa, G.; Ramos, J. M. *J. Chem. Soc., Dalton Trans.* **1990**, 2931.

at 40 °C for 24 h (see Table 2). Then two drops of water were added to hydrolyze the excess of organolithium reagent, and the volatiles were removed *in vacuo*. Once the reaction mixture had been hydrolyzed, the filtrations on dry Celite and purification procedures were performed under normal atmosphere. The workup procedure is detailed below for each compound. All the compounds obtained are air-stable solids.

Arylation of *trans*-[PdCl$_2$(tht)$_2$]. The black residue was extracted with 30 mL of CH_2Cl_2 and filtered. Hexane (15 mL) was added to the yellow filtrate, and the solution was concentrated *in vacuo* and cooled to −20 °C. The pale yellow crystals thus obtained were decanted, washed with hexane (3 × 5 mL), and dried *in vacuo*, yielding *trans*-[Pd(Fmes)$_2$(tht)$_2$], **2**. Anal. Calcd for $C_{26}H_{20}F_{18}PdS_2$: C, 36.96; H, 2.39. Found: C, 36.72; H, 2.44. ^{1}H NMR ($CDCl_3$): δ 7.90 (s, 4 H, $C_6H_2(CF_3)_3$), 2.27 (m, 8 H, H^2 of tht), 1.72 (m, 8 H, H^3 of tht). IR: 1622 m, 1571 w, 1300 vs, 1283 vs, 1175 vs br, 1130 vs br, 1070 s, 1012 m, 912 m, 852 m, 836 m, 756 m, 686 s, 667 m, 441 m, 243 m.

When the reactant ratio used was 1:2 (see Table 2), concentration of the mother liquor solution and cooling to −20 °C gave an orange solid, which was decanted, washed with hexane (3 × 5 mL), and dried *in vacuo*, yielding *trans*-[Pd(Fmes)Cl(tht)$_2$], **1**. Anal. Calcd for $C_{17}H_{18}ClF_9PdS_2$: C, 34.45; H, 3.02. Found: C, 34.17; H, 3.03. ^{1}H NMR ($CDCl_3$): δ 7.88 (s, 2 H, $C_6H_2(CF_3)_3$), 2.97 (m, 8 H, H^2 of tht), 2.00 (m, 8 H, H^3 of tht). IR: 1621 m, 1569 w, 1297 s, 1277 vs, 1193 vs, 1181 vs, 1140 vs, 1112 vs, 1087 s, 1027 m, 952 w, 916 m, 883 w br, 851 m, 834 m, 802 vw, 754 m, 693 m, 683 s, 520 vs, 468 w, 437 w, 290 w br, 230 m.

X-ray Crystallographic Analysis of *trans*-[Pd(Fmes)$_2$(tht)$_2$], 2. Suitable crystals of **2** were grown by slow diffusion of a concentrated dichloromethane solution of the complex into hexane at room temperature. A crystal of **2** (approximate dimensions 0.40 × 0.40 × 0.40 mm) was mounted in a glass fiber and held in place with epoxy glue. All diffraction measurements were made at room temperature on a Siemens R3m diffractometer, using graphite monochromated Mo Kα X-radiation. Unit cell dimensions were determined from 20 centered reflections in the range $16.0 < 2\theta < 29.3°$. Diffracted intensities were measured in a unique quadrant of reciprocal space for $3.0 < 2\theta < 50.0°$ by ω Wyckoff scans. Three check reflections remeasured after every 150 ordinary data showed no decay and variation of ±2% over the period of data collection. Of the 5701 intensity data (other than checks) collected, 5205 unique observations remained after averaging of duplicate and equivalent measurements ($R_{int} = 0.044$) and deletion of systematic absences all of which were used in structure solution and refinement. An absorption correction was applied based on 504 azimuthal scan data (maximum and minimum transmission coefficients were 0.294 and 0.205). Lorentz and polarization corrections were applied.

The structure was solved by Patterson and Fourier methods and refined using the SHELXL-93 program.[29] All non-hydrogen atoms were assigned anisotropic displacement parameters. All hydrogen atoms were constrained to idealized geometries and their positions refined riding on their parent carbon atoms with a common thermal isotropic parameter. In four of the six CF_3 groups [C(8), C(16), C(17), and C(18)] the fluorine atoms show a rotational disorder over two set of positions related by a pseudo-2-fold axis approximately coincident with the C_{ipso}−CF_3 bond. In the four cases the occupancy of one of the sets is clearly bigger than for the other [0.83(1) in the case of the C(8) group, 0.91(1) for C(16), 0.68(1) for C(17), and 0.81(1) for C(18)]. The geometry of all the CF_3 groups was restrained using the DFIX and SAME instructions. Common thermal parameters for the pseudo-2-fold related fluorine atoms in the disordered CF_3 groups were applied using the EADP instruction. Full-matrix least squares refinement of this model (465 parameters) on F^2 converged to final residual indices $R1 = 0.065$, $wR2 = 0.0169$ [for the 4411 reflections with $I > 2\sigma(I)$], and $S = 1.06$ for all data. Weights, w, were set equal to $[\sigma_c^2(F_o^2) + (aP)^2]^{-1}$, where $\sigma_c^2(F_o^2)$ = variance in F_o^2 due to counting statistics, $P = [\max(F_o^2,0) + 2F_c^2]/3$, and $a = 0.15$ was chosen to minimize the variation in S as a function of F_o. Final difference electron density maps showed features in the range +2.55 to −1.58 e Å^{-3}; the largest features (2.55, 2.45, 1.09, and 1.01 e Å^{-3}) lie within 1 Å of the metal atom. These and further details are listed in Table 5, while Table 6 lists the final atomic positional parameters for the freely refined atoms.

Table 5. Crystal Data and Structure Refinement for 2 and 6

	compd **2**	compd **6**
empirical formula	$C_{26}H_{20}F_{18}PdS_2$	$C_{28}H_{12}F_{18}N_2Pd$
fw	844.94	824.80
temp (K)	293	293
wavelength (Å)	0.710 73	0.710 73
cryst system	monoclinic	monoclinic
space group	$P2_1/n$	$P2_1/n$
unit cell dimens	a = 11.976(5) Å	a = 9.029(5) Å
	b = 15.257(4) Å	b = 18.824(7) Å
	c = 16.299(5) Å	c = 16.603(5) Å
	β = 93.85(3)°	β = 96.23(4)°
V (Å^3)	2971.3(17)	2805(2)
Z	4	4
D_{calc} (Mg/m^3)	1.896	1.953
abs coeff (mm^{-1})	0.900	0.806
F(000)	1664	1608
crystal size (mm)	0.40 × 0.40 × 0.40	0.50 × 0.40 × 0.45
2θ range for data collcn (deg)	3−50	3−50
index ranges	$0 \le h \le 14$	$0 \le h \le 10$
	$0 \le k \le 18$	$0 \le k \le 22$
	$-19 \le l \le 19$	$-19 \le l \le 19$
reflcns collcd	5470	5266
indepdt reflcns	5205 [R(int) = 0.0435]	4934 [R(int) = 0.0203]
refinement method	full-matrix least-squares on F^2	
data/restraints/params	5199/54/465	4932/12/533
goodness-of-fit on F^2	1.055	1.370
final R indices [$I > 2\sigma(I)$][a]	$R1$ = 0.0650	$R1$ = 0.0284
	w$R2$ = 0.1692	w$R2$ = 0.0735
R indices (all data)[a]	$R1$ = 0.0746	$R1$ = 0.0363
	w$R2$ = 0.1962	w$R2$ = 0.0775
largest diff peak and hole (e Å^{-3})	2.55 and −1.58	0.43 and −0.37

[a] $R1 = \sum||F_o| - |F_c||/\sum|F_o|$; $wR2 = [\sum[w(F_o^2 - F_c^2)^2/\sum[w(F_o^2)^2]]^{1/2}$; goodness-of-fit = $[\sum w(F_o^2 - F_c^2)^2/(\text{no. reflcns} - \text{no. params})]^{1/2}$.

Arylation of *trans*-[PdCl$_2$(PPh$_3$)$_2$]. The brown residue was extracted with 20 mL of toluene and filtered. Concentration of the brown filtrate and cooling to −20 °C gave white crystals, which were decanted, washed with hexane (3 × 10 mL), and dried *in vacuo*, yielding *trans*-[Pd(Fmes)Cl(PPh$_3$)$_2$], **3**. Anal. Calcd for $C_{45}H_{32}ClF_9P_2Pd$: C, 57.04; H, 3.40. Found: C, 57.18; H, 3.51. ^{1}H NMR ($CDCl_3$, −60 °C): δ 8.05 (m, 8 H, *ortho*-C_6H_5), 7.50 (m, 12 H, *meta*- and *para*-C_6H_5), 7.08 (s, 2 H, $C_6H_2(CF_3)_3$), 7.01 (t, J 7.4 Hz, 2 H, *para*-C_6H_5), 6.76 (t, J 7.6 Hz, 4 H, *meta*-C_6H_5), 6.40 (m, 4 H, *ortho*-C_6H_5). ^{31}P{^{1}H} NMR (121.4 MHz, $CDCl_3$, room temperature): δ 21.3 (sept, J_{PF} 5.6 Hz). IR: 1621 w, 1576 vw, 1373 s, 1284 vs, 1260 s, 1180 vs, 1131 vs, 1094 s, 1023 w, 1002 vw, 908 m, 833 vw, 744 s, 694 s, 518 vs, 442 s br, 302 s br.

Spin Saturation Transfer (SST) Experiment. A *ca.* 0.02 M solution of **3** in carefully degassed $CDCl_3$ was prepared in a 5 mm NMR tube. The experiments were carried out at 208.8 K. T_1 (0.9 s) was determined by the 180−τ−90 pulse sequence. The decoupler power was adjusted so that complete saturation of the peak was observed after irradiation for at least five T_1 (10 s). The extent of saturation transfer was ascertained by examining difference spectra resulting from subtraction of data collected with and without saturation at the resonances of the *ortho*-phenylic hydrogens (A = 6.40 or B = 8.05 ppm). A SST

(29) SHELXTL version 5.03, Siemens Analytical Xray, Madison, WI, 1994.

Table 6. Atomic Coordinates ($\times 10^4$) and Equivalent Isotropic Displacement Parameters (Å^2 $\times 10^3$) for 2, with *U*(eq) Defined as One-Third of the Trace of the Orthogonalized U_{ij} Tensor

	x	*y*	*z*	*U*(eq)
Pd	1084(1)	2182(1)	1228(1)	32(1)
S(1)	1293(1)	2481(1)	2626(1)	43(1)
S(2)	630(1)	1880(1)	−145(1)	45(1)
C(1)	2479(4)	1362(3)	1258(3)	36(1)
C(2)	2435(4)	443(3)	1344(3)	38(1)
C(3)	3365(4)	−97(4)	1328(3)	44(1)
C(4)	4403(4)	266(4)	1251(3)	47(1)
C(5)	4518(4)	1155(4)	1181(3)	45(1)
C(6)	3573(4)	1694(3)	1190(3)	40(1)
C(7)	1335(5)	−7(3)	1432(3)	48(1)
F(1)	808(3)	282(3)	2078(2)	68(1)
F(2)	614(3)	106(2)	774(2)	67(1)
F(3)	1434(3)	−872(2)	1543(3)	71(1)
C(8)	5393(5)	−312(4)	1216(4)	67(2)
F(4′)[a]	6099(21)	45(19)	1804(16)	95(2)
F(5′)[a]	5342(22)	−1090(11)	1543(21)	88(2)
F(6′)[a]	5980(26)	−331(29)	570(13)	160(5)
F(4)[b]	5810(8)	−579(8)	1927(3)	160(5)
F(5)[b]	5167(5)	−1075(3)	814(5)	95(2)
F(6)[b]	6191(5)	15(4)	791(5)	88(2)
C(9)	3770(4)	2660(4)	1096(4)	53(1)
F(7)	4847(3)	2852(3)	1034(4)	97(2)
F(8)	3437(4)	3123(3)	1718(3)	83(1)
F(9)	3249(4)	2988(3)	419(3)	82(1)
C(10)	−313(4)	3035(3)	1193(3)	36(1)
C(11)	−1435(4)	2752(3)	1203(3)	38(1)
C(12)	−2341(4)	3330(4)	1223(3)	45(1)
C(13)	−2173(4)	4212(4)	1223(3)	45(1)
C(14)	−1110(5)	4539(4)	1203(3)	45(1)
C(15)	−203(4)	3962(3)	1187(3)	37(1)
C(16)	−1780(4)	1806(4)	1171(3)	49(1)
F(10′)[c]	−1925(60)	1578(35)	1936(11)	110(3)
F(11′)[c]	−2742(27)	1677(30)	755(36)	79(2)
F(12′)[c]	−1078(40)	1235(28)	886(42)	97(2)
F(10)[d]	−2583(5)	1632(3)	1657(5)	97(2)
F(11)[d]	−2185(9)	1584(4)	421(4)	110(3)
F(12)[d]	−991(3)	1226(3)	1356(5)	79(2)
C(17)	−3143(5)	4821(4)	1252(4)	61(2)
F(13′)[e]	−3253(21)	5336(20)	603(14)	125(4)
F(14′)[e]	−2952(22)	5383(19)	1854(17)	144(5)
F(15′)[e]	−4083(11)	4474(11)	1441(22)	112(3)
F(13)[f]	−2910(6)	5656(4)	1291(11)	112(3)
F(14)[f]	−3707(11)	4709(9)	1908(8)	125(4)
F(15)[f]	−3904(10)	4712(10)	631(8)	144(5)
C(18)	903(4)	4414(3)	1164(3)	46(1)
F(16′)[g]	847(19)	5166(13)	1570(18)	79(2)
F(17′)[g]	1754(17)	4011(17)	1552(21)	101(3)
F(18′)[g]	1279(19)	4576(25)	450(8)	86(2)
F(16)[h]	853(4)	5255(3)	976(7)	101(3)
F(17)[h]	1564(5)	4323(6)	1839(3)	86(2)
F(18)[h]	1535(5)	4086(5)	596(4)	79(2)
C(19)	162(5)	1980(5)	3158(4)	57(1)
C(20)	693(8)	1692(8)	3981(5)	96(3)
C(21)	1832(9)	1450(9)	3895(5)	125(5)
C(22)	2392(6)	1863(6)	3219(4)	68(2)
C(23)	1708(6)	1373(5)	−720(4)	69(2)
C(24)	1841(11)	1944(9)	−1456(6)	130(5)
C(25)	946(10)	2562(7)	−1584(5)	103(3)
C(26)	557(8)	2845(5)	−785(4)	78(2)

[a] Occupancy 0.17. [b] Occupancy 0.83. [c] Occupancy 0.09. [d] Occupancy 0.91. [e] Occupancy 0.32. [f] Occupancy 0.68. [g] Occupancy 0.19. [h] Occupancy 0.81.

experiment was performed by irradiating one of the resonances and observing magnetization transfer into the other signal after variable delays (0.05−0.9 s). Plots of $[M_z(H) - M_\infty(H)]$ *vs t* were analyzed by standard least-square fitting procedures. Values of $1/\tau_1(H)$ thus obtained were used to calculate k_{obs}.[30] ($k_{obs}(A) = 0.124 \pm 0.013$ s^{-1}; $k_{obs}(B) = 0.066 \pm 0.013$ s^{-1}). Rates of chemical exchange (k_{chem}) were obtained as previously outlined for a two-site exchange process between sites of population 1 and 2 [$k_{chem} = (3/2)k_{obs}(A) = 3k_{obs}(B)$].[31] The chemical rate constants thus obtained from SST experiments

Table 7. Atomic Coordinates ($\times 10^4$) and Equivalent Isotropic Displacement Parameters (Å^2 $\times 10^3$) for 6, with *U*(eq) Defined as One-Third of the Trace of the Orthogonalized U_{ij} Tensor

	x	*y*	*z*	*U*(eq)
Pd	9164(1)	2768(1)	8165(1)	31(1)
C(1)	8959(3)	2150(1)	9150(2)	33(1)
C(2)	9629(3)	2263(1)	9954(2)	38(1)
C(3)	9487(3)	1790(2)	10581(2)	46(1)
C(4)	8691(4)	1175(2)	10452(2)	48(1)
C(5)	8063(3)	1027(2)	9677(2)	46(1)
C(6)	8209(3)	1490(1)	9047(2)	37(1)
C(7)	10597(3)	2890(2)	10156(2)	52(1)
F(1)	9880(3)	3504(1)	10109(1)	79(1)
F(2)	11297(3)	2863(1)	10910(1)	79(1)
F(3)	11694(3)	2937(1)	9676(1)	82(1)
C(8)	8523(5)	669(2)	11128(2)	74(1)
F(4)[a]	9660(10)	690(5)	11702(4)	103(3)
F(5)[a]	8635(16)	−9(3)	10886(4)	115(3)
F(6)[a]	7369(13)	718(9)	11458(10)	177(5)
F(4′)[b]	7394(19)	233(8)	10947(6)	123(5)
F(5′)[b]	9708(13)	314(11)	11316(13)	176(8)
F(6′)[b]	8189(22)	1016(5)	11779(5)	115(5)
C(9)	7526(3)	1186(2)	8249(2)	46(1)
F(7)	6135(2)	961(1)	8307(1)	88(1)
F(8)	8273(3)	615(1)	8059(1)	84(1)
F(9)	7438(2)	1602(1)	7615(1)	61(1)
C(10)	7975(3)	3604(1)	8511(2)	34(1)
C(11)	8697(3)	4266(1)	8638(2)	38(1)
C(12)	7956(4)	4880(2)	8828(2)	45(1)
C(13)	6448(3)	4868(2)	8878(2)	45(1)
C(14)	5675(4)	4248(2)	8723(2)	42(1)
C(15)	6422(3)	3631(1)	8547(2)	35(1)
C(16)	10310(3)	4417(2)	8528(2)	50(1)
F(10)	11178(2)	3871(1)	8447(2)	71(1)
F(11)	10385(2)	4807(1)	7858(2)	89(1)
F(12)	10965(2)	4807(1)	9124(2)	93(1)
C(17)	5686(5)	5545(2)	9068(2)	65(1)
F(13)[b]	5537(27)	5865(7)	8502(12)	242(13)
F(14)[b]	6159(14)	5796(5)	9801(4)	109(5)
F(15)[b]	4325(10)	5443(6)	9261(5)	58(3)
F(13′)[a]	4270(8)	5481(5)	9089(6)	143(5)
F(14′)[a]	5874(10)	6095(3)	8551(5)	99(2)
F(15′)[a]	6330(9)	5848(4)	9738(5)	150(5)
C(18)	5463(3)	2994(2)	8343(2)	44(1)
F(16)	5729(2)	2456(1)	8858(1)	61(1)
F(17)	4011(2)	3130(1)	8323(2)	73(1)
F(18)	5643(2)	2733(1)	7610(1)	64(1)
N(1)	9242(3)	3189(1)	6992(1)	38(1)
N(2)	10749(2)	2099(1)	7717(1)	37(1)
C(19)	8357(4)	3687(2)	6630(2)	49(1)
C(20)	8316(4)	3841(2)	5821(2)	63(1)
C(21)	9216(5)	3465(2)	5366(2)	68(1)
C(22)	10138(4)	2953(2)	5725(2)	58(1)
C(23)	10135(3)	2823(1)	6544(2)	39(1)
C(24)	11088(3)	2274(1)	6974(2)	38(1)
C(25)	12268(4)	1960(2)	6650(2)	50(1)
C(26)	13098(4)	1445(2)	7080(2)	59(1)
C(27)	12726(4)	1255(2)	7826(2)	57(1)
C(28)	11565(3)	1596(2)	8123(2)	47(1)

[a] Occupancy 0.4. [b] Occupancy 0.6.

irradiating either A or B signals are essentially equal ($k_{chem}(A) = 0.186 \pm 0.019$ s^{-1}; $k_{chem}(B) = 0.20 \pm 0.04$ s^{-1}). The free energies of activation were calculated by using the Eyring equation, averaging 12.8 kcal mol^{-1} ($\Delta G^{\ddagger}(A) = 12.77 \pm 0.10$ kcal mol^{-1}; $\Delta G^{\ddagger}(B) = 12.74 \pm 0.19$ kcal mol^{-1}). Uncertainties in the rate constants were calculated from the residuals of the best-fit line drawn to the data, assuming a ±0.01 error in the

(30) (a) Sandström, J. *Dynamic NMR Spectroscopy*; Academic Press; London, 1982; p 53 and references therein. (b) Faller, J. W. In *Determination of Organic Structures by Physical Methods*; Nachod, F. C., Zuckerman, J. J., Eds.; Academic Press: New York, 1973; Vol. 5, Chapter 5. (c) Sanders, J. K. M.; Hunter, B. K. *Modern NMR Spectroscopy, A Guide for Chemists*; Oxford University Press: Oxford, U.K., 1987; p 225.

(31) Green, M. L. H.; Wong, L.-L.; Sella, A. *Organometallics* **1992**, *11*, 2660.

integrals. The temperature was calibrated with a CH_3OH sample before and after the experiment and is accurate to within 0.1 °C. The uncertainties in rates and temperature were propagated to find the uncertainty in $\Delta G^{\ddagger}$.

Arylation of [PdCl$_2$(COD)]. The gray residue was extracted with 30 mL of CH_2Cl_2 and filtered. Hexane (15 mL) was added to the yellow filtrate, and the solution was concentrated *in vacuo* and cooled at −20 °C. The pale yellow crystals obtained were decanted, washed with hexane (3 × 10 mL), and dried *in vacuo*, yielding [Pd(Fmes)Cl(COD)], **4**. Anal. Calcd for $C_{17}H_{14}ClF_9Pd$: C, 38.44; H, 2.66. Found: C, 38.36; H, 2.67. ^{1}H NMR ($CDCl_3$): δ 7.86 (s, 2 H, $C_6H_2(CF_3)_3$), 6.25 (m, 2 H, $H_{olefinic}$ of COD), 5.43 (m, 2 H, $H_{olefinic}$ of COD), 2.79 (m, 4 H, $H_{aliphatic}$ of COD), 2.59 (m, 4 H, $H_{aliphatic}$ of COD). IR: 1711 vw, 1621 w, 1301 s, 1284 vs, 1264 s, 1190 vs, 1123 vs, 1023 m, 914 m, 781 m br, 684 m, 568 w br, 437 m, 323 m, 300 w.

Arylation of [PdCl$_2$(bipy)]. The green residue was extracted in a Soxhlet apparatus with 200 mL of refluxing toluene. The brown solution obtained was filtered and concentrated *in vacuo*. Cooling at −20 °C gave yellow microcrystals, which were decanted, washed with hexane (3 × 10 mL), and dried *in vacuo*, yielding [Pd(Fmes)Cl(bipy)], **5**. Anal. Calcd for $C_{19}H_{10}ClF_9N_2Pd$: C, 39.41; H, 1.74; N, 4.84. Found: C, 39.56; H, 1.90; N, 5.03. ^{1}H NMR ($CDCl_3$): δ 9.37 (d, J 4.3 Hz, 1 H, H^6 of bipy), 8.08 (m, 4 H, H^3, 2 H^5 and H^6 of bipy), 7.92 (s, 2 H, $C_6H_2(CF_3)_3$), 7.64 (m, 1 H, H^4 of bipy), 7.57 (d, J 5.5 Hz, 1H, H^3 of bipy), 7.32 (ddd, J 7.3, 5.6, and 1.8 Hz, 1H, H^4 of bipy). IR: 1619 m, 1603 m, 1571 m, 1300 vs, 1282 vs, 1265 vs, 1188 vs, 1128 m, 1106 m, 1085 m, 1036 m, 914 m, 854 m, 835 m, 767s, 755 w, 696 m, 684 s, 667 w, 649 w, 474 w, 439 w, 418 w, 396 vw, 374 vw, 340 m, 252 w.

Concentration of the mother liquors and cooling to −20 °C afforded an off-white solid, which was decanted, washed with hexane (3 × 5 mL), and dried *in vacuo*, yielding [Pd(Fmes)$_2$(bipy)], **6**. When the reaction was carried out with 4-fold excess of Li(Fmes), the green residue was extracted with 30 mL of CH_2Cl_2 and filtered. This yellow solution was concentrated and chromatographed on a silica gel column using CH_2Cl_2 as eluant. The solution obtained was evaporated to dryness and the yellow residue was recrystallized from acetone/hexane to give **6**. Anal. Calcd for $C_{28}H_{12}F_{18}N_2Pd$: C, 40.78; H, 1.47; N, 3.40. Found: C, 40.88; H, 1.65; N, 3.62. ^{1}H NMR ($CDCl_3$): δ 8.12 (d, J 7.9 Hz, 2 H, H^6 of bipy), 8.04 (ddd, J 7.8, 7.8, and 1.6 Hz, 2 H, H^5 of bipy), 7.79 (s, 4 H, $C_6H_2(CF_3)_3$), 7.64 (d, J 5.3 Hz, 2 H, H^3 of bipy), 7.36 (ddd, J 7.1, 5.5, and 1.3 Hz, 2 H, H^4 of bipy). IR: 1620 s, 1607 w, 1565 m, 1278 vs, 1192 s, 1163 vs, 1130 vs, 1098 vs, 1073 s, 1031 m, 1015 m, 923 m, 907 m, 852 m, 831 m, 761 s, 749 m, 692 m, 686 s, 663 w, 642 vw, 459 w, 437 w, 373 vw.

X-ray Crystallographic Analysis of [Pd(Fmes)$_2$(bipy)], 6. Suitable crystals of **6** were grown by slow diffusion of a concentrated acetone solution of the complex into hexane at room temperature All diffraction measurements were made with a Siemens four-circle R3m diffractometer, using graphite monochromated Mo Kα X-radiation on a single crystal (approximate dimensions 0.50 × 0.40 × 0.45 mm) mounted on a glass fiber with superglue. Unit cell dimensions were determined from 25 centered reflections in the range $15 < 2\theta < 30°$. A total of 5545 diffracted intensities (including checks) were measured in a unique quadrant of reciprocal space for $3.0 < 2\theta < 50.0°$ by Wyckoff ω scans. Three check reflections remeasured after every 200 ordinary data showed no decay and *ca.* ±2% variation over the period of data collection. Of the 5432 noncheck intensity data collected, 4932 unique observations remained after averaging of duplicate and equivalent measurements ($R_{int} = 0.0203$) and deletion of systematic absences and were retained for use in structure solution and refinement. An absorption correction was applied in the basis of 306 azimuthal scan data; maximum and minimum transmission coefficients were 0.829 and 0.696, respectively. Lorentz and polarization corrections were applied.

The structure was solved by Patterson and Fourier methods and refined using the SHELXL-93 program.[29] All nonhydrogen atoms were assigned anisotropic displacement parameters and, except for the disordered CF_3 groups in the *para* position on the aryl rings, refined without positional constraints. For the disordered CF_3 groups restraints were applied so that C−F distances were close to 1.33 Å and F···F distances close to 2.12 Å. Hydrogen atoms were located in the Fourier maps and freely refined with a common thermal isotropic parameter. Occupancies of the fluorine atoms of the *para*-CF_3 groups were initially refined and then fixed (at 0.4 and 0.6 for F(4−6, 13′−15′) and F(4′−6′, 13−15), respectively). Refinement of the 533 least-squares variables converged smoothly to residual indices $R1 = 0.028$, w$R2 = 0.0074$ [for the 4266 reflections with $I > 2\sigma(I)$], and $S = 1.37$ for all data. Weights, w, were set equal to $[\sigma_c^2(F_o^2) + (aP)^2]^{-1}$, where $\sigma_c^2(F_o^2)$ = variance in F_o^2 due to counting statistics, $P = [\max(F_o^2,0) + 2F_c^2]/3$, and $a = 0.04$ was chosen to minimize the variation in S as a function of F_o. Final difference electron density maps showed no features outside the range +0.43 to −0.37 e Å^{-3}, the largest features being close to the fluorine atoms. Table 5 reports the details of the structure analysis, and Table 7, the atomic positional parameters.

Acknowledgment. The authors in Valladolid thank the DGICYT of Spain for financial support (Project PB93-0222). The collaboration was under the sponsorship of the European Community (Contract CHRX-CT93-0147 (DG 12 DSCS)). A.M. thanks the Spanish Ministerio de Educación y Ciencia for a FPU (Becas en el extranjero) grant. We also thank Asunción Muñoz (Universidad de Burgos, Burgos, Spain) for performing the electrochemical experiments.

Supporting Information Available: For the crystal structures of **2** and **6**, complete tables of bond distances and angles, anisotropic thermal parameters for the non-hydrogen atoms, and hydrogen atom positions and isotropic thermal parameters (6 pages). Ordering information is given on any current masthead page.

OM950851T